Effect of cooling rates on solidification and microstructure of rapidly solidified $Mg_{57}Zn_{37}Y_6$ quasicrystal alloy

Min Xu and Xinying Teng[a)]
School of Materials Science and Engineering, University of Jinan, Jinan 250022, Shandong Province, People's Republic of China

Jiwei Geng
State Key Laboratory of Metal Matrix Composites, Shanghai Jiao Tong University, Shanghai 200240, People's Republic of China

(Received 14 May 2015; accepted 28 August 2015)

The influence of cooling rates on the solidification and microstructure of rapidly solidified quasicrystal alloys with a nominal compositions of $Mg_{57}Zn_{37}Y_6$ (at.%) prepared by melt spinning method was investigated. The microstructure, phase constitution, phase transition, and phase structure of the alloys were examined by means of scanning electron microscopy, x-ray diffraction, energy dispersive spectrometer, differential scanning calorimetry, and transmission electron microscopy. The results show that rapid solidification refines and homogenizes the microstructure of $Mg_{57}Zn_{37}Y_6$ alloys, compared to the conventionally-cast master alloy. With the increasing cooling rate of rapid solidification, the thickness of the ribbon decreases greatly and a larger amount of I-phase can be formed. α-Mg, MgZn, and icosahedral phases are found in the as-cast alloy, but the MgZn phase is absent from rapidly solidified alloys. The I-phase in both as-cast and rapidly solidified alloys can precipitate directly from the melt during the solidification process. A higher cooling rate can lead to a large degree of supercooling, resulting in a decreased phase transition temperature and a large number of icosahedral short-range orders (ISROs). ISROs can act as templates in liquid and promote the nucleation of I-phase.

I. INTRODUCTION

Magnesium alloy is known as "the most promising structure material in 21st century" with a series of advantages such as low density, high specific stiffness and strength, strong electromagnetic shielding performance, and superior damping capacity performance.[1] Since Shechtman et al.[2] discovered the quasicrystal in a rapidly solidified Al–Mn alloy, icosahedral quasicrystal phase (I-phase) that have the quasiperiodic lattice structure has been reported in many alloy systems later on. The stable I-phase ($Mg_3Zn_6Y_1$) in Mg–Zn–Y alloy was first discovered by Luo et al.[3] and confirmed by Tsai et al.,[4] which initiated the research on structure, properties, formation mechanism and growth morphology of the I-phase in as-cast Mg–Zn–Y alloy. It has been reported that the I-phase demonstrates many attractive properties such as low interfacial energy, high strength, high thermal conductivity, and low friction coefficient,[5–8] which makes the Mg–Zn–Y alloys a potential candidate for developing advanced magnesium alloys.

Previous investigations revealed that rapid solidification technology can produce metastable and novel structures, as well as fine grains in alloys.[9–11] Many researchers have been focused on the rapid solidification of Mg–Zn–Y series alloys due to their excellent mechanical properties obtained through rapid solidification and extrusion.[12,13] Great efforts have also been taken on studying the I-phase performing as a strengthening phase in Mg–Zn–Y alloy. Recently, some researchers concentrated their attentions on the differences of microstructure between as-cast and as-quenched I-phase in Mg–Zn–Y alloy.[14–16] However, only single cooling rate was used in the studies. It is well known that the microstructure of rapidly solidified alloys bears strong relationship with the cooling rates. Research on the difference of microstructure and solidification process between the traditional solidified; however, the relationship between different cooling rates and the growth mechanism of I-phase in rapidly solidified Mg–Zn–Y alloy has only rarely studied. Liu et al.[17] have carried on the study of icosahedral phase in a rapidly solidified Al–Fe–Ce alloy under different cooling rates, providing a detailed and systemic work.

The growth morphology of icosahedral quasicrystal greatly depends on the nature of the quasiperiodicity, point group symmetry, and atomic attachment kinetics, especially for rapidly solidified Mg–Zn–Y alloy of different cooling rates.[14–16,18,19] Therefore, studying the effect of cooling rates on the solidification and microstructure of rapidly solidified $Mg_{57}Zn_{37}Y_6$ quasicrystal alloy can contribute to optimizing and controlling alloy microstructure.

Contributing Editor: Yang-T. Cheng
[a)]Address all correspondence to this author.
e-mail: mse_tengxy@ujn.edu.cn
DOI: 10.1557/jmr.2015.283

II. EXPERIMENTAL PROCEDURE

The Mg–Zn–Y quasicrystal alloy with a nominal composition of $Mg_{57}Zn_{37}Y_6$ (at.%) was prepared using high pure Mg (purity > 99.9 wt%), Zn (purity > 99.9 wt%), and Mg–(29.57 wt%) Y master alloy. Mg and Mg–29.57 wt% Y master alloy were added to the crucible, and Zinc was subsequently added to reduce the burning of alloy elements at 710 °C. All the materials were melted at 740 °C for 30 min with a frequent stirring, and then cast into a steel mold with a diameter of 12 mm preheated at 200 °C followed by a slow cooling under atmosphere. The rapidly solidified alloy ribbons were prepared by melt spinning (planar flow cast on a Cu wheel) at different wheel speeds, 5–10 m/s. The obtained ribbons were 2.0–3.5 mm wide and 141–265 μm thick. The grain size was measured by the standard linear intercept method using an Olympus stereomicroscope. The volume fraction of the secondary phase in the alloy was determined by Lmage-Pro Plus 6.0 and 10 images were used to calculate the average volume fractions.

The microstructure of the conventionally-cast alloy and the rapidly solidified ribbons were observed by scanning electron microscopy (SEM; QUANTA FEG250, FEI Company, Hillsboro, Oregon) equipped with energy dispersive spectrum (EDS; X-MAX50, Oxford Instruments, Oxfordshire, UK) for analyzing the local chemical compositions of different phases. The crystallographic features were investigated by high-resolution transmission electron microscopy (TEM) (JEM-2100, JEOL, Tokyo, Japan). The phases were determined by x-ray diffraction (XRD; D8-ADVANCE, Bruker, Karlsruhe, Germany) with Cu K_α radiation, and the transition behavior of phase was analyzed with differential scanning calorimetry (DSC; STA409EP, Netzsch Instruments Inc., Burlington, Massachusetts). The samples were immersed for 3–5 s in an etchant (5 mL HNO_3, 75 mL ethanol and 20 mL deionized water) for a further morphology observation. The samples for TEM were dimpled down to about 20 μm in the center by ion milling after mechanically polishing.

III. RESULTS AND DISCUSSION

A. The effect of cooling rates on the thickness of rapidly solidified $Mg_{57}Zn_{37}Y_6$ ribbons

Table I shows the thickness of the two specimens at different wheel speeds for rapidly solidification of $Mg_{57}Zn_{37}Y_6$ ribbons. The thickness of two specimens is found to decrease with the increasing wheel speed, as shown in Table I. The thickness of rapidly solidified alloys bears strong relationship with the distance which is moved by the melt until it solidifies. However, many processing parameters can influence the distance, such as wheel speed, gas ejection pressure, and melting temperature.[20,21] When both of the gas ejection pressure and melting temperature are stable, the quantity and thermal physical properties of the melt are constant. Therefore, the length moved by the melt is larger at higher wheel speed, which leads to the decrease of the thicknesses of ribbon.

TABLE I. Average ribbon thickness of rapidly solidified $Mg_{57}Zn_{37}Y_6$ alloys at different wheel speeds.

Sample	Wheel speeds (r/min)	Wheel speeds (m/s)	Thickness (μm)
As-cast alloy	0	0	...
Specimen 1	400	5.02	265
Specimen 2	800	10.04	141

The cooling rate of rapidly solidified ribbons increases linearly with the wheel speed,[22] it is also inversely proportional to the square of the thickness of rapidly solidified Magnesium alloy ribbons, as showed in Eq. (1).[23] For wheel speeds in the range from 5 to 10 m/s, the heat transfer velocity of the melt decreases with the increase of wheel speeds. According to Eq. (1), the cooling rates are approximately 2.35×10^5 and 8.29×10^5 K/s at the wheel speeds of 5 and 10 m/s, respectively.

$$\frac{\partial T}{\partial t} = 0.016475x^{-2} \quad , \tag{1}$$

where $\frac{\partial T}{\partial t}$ and x are the cooling rate and the ribbon thickness, respectively. The constant of 0.016475 is used in the calculation based on a series of work.[23]

B. The effect of cooling rates on the microstructure of rapidly solidified $Mg_{57}Zn_{37}Y_6$ ribbons

Figure 1 shows the XRD patterns for both conventionally-cast alloy and the rapidly solidified samples of $Mg_{57}Zn_{37}Y_6$ alloy. Three phases are identified in conventionally-cast alloy shown in Fig. 1(a),

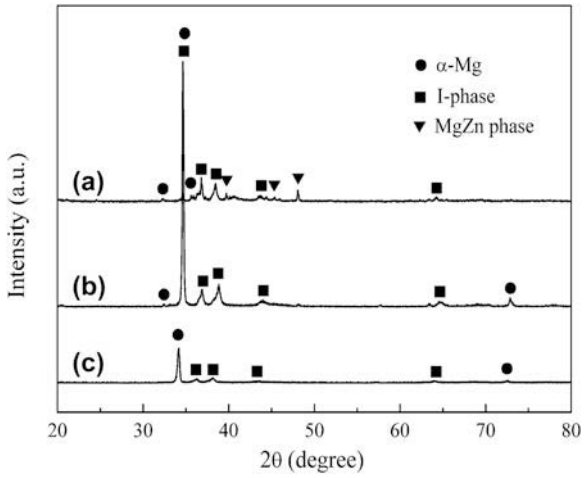

FIG. 1. XRD patterns of the $Mg_{57}Zn_{37}Y_6$ alloy solidified at different wheel speeds: (a) conventionally-cast alloy, (b) 400 r/min, and (c) 800 r/min.

and those are α-Mg, MgZn phase, and I-phase. However, only two phases: α-Mg phase and I-phase, are found in the both rapidly solidified specimens, shown in Figs. 1(b) and 1(c), respectively.

Figure 2 shows the SEM images under backscattered model of the $Mg_{57}Zn_{37}Y_6$ alloy solidified at different cooling rates. In Fig. 2(a), most of the primary I-phases have a pentagonal core, and five branches form along the direction of the pentagonal corner. The bright petal-like I-phases and I-phase particles surrounded by low-temperature phase MgZn and little lamellar eutectic structures (I-phase + α-Mg) as laths in the transformed lamellas,[24] as marked in Fig. 2(a) by arrows, are distributed in the matrix. The pentagonal core is obviously smaller than the five branches, in the result of limitation by the growth space and the interfacial energy. However, the I-phase eutectic structures and MgZn phases are absent from specimen 1, and there are many more primary I-phases in Fig. 2(b), which shows the microstructure of rapidly solidified $Mg_{57}Zn_{37}Y_6$ alloy at a wheel speed of 400 r/min. As can be seen, the microstructure of this specimen is composed of two phases. The dominant phase I-phases can exist both as a pentagonal core with five branches and particles morphology. Figure 2(c) shows the microstructure of the rapidly solidified $Mg_{57}Zn_{37}Y_6$ alloy with higher wheel speed (800 r/min). As can be seen in Figs. 2(b) and 2(c), there exist no apparent differences among the SEM images of the rapidly solidified alloy samples, indicating the fact that rapid solidification can make the alloys homogenized significantly. However, with the increasing cooling rate, the volume fraction of second phase increases, which is believed to result from solidification under different cooling rates. Compared with the alloy produced at a lower cooling rate, the grain size of second phase decreases dramatically with a higher wheel speed. The volume fraction and the grain size of phases measured by Olympus stereomicroscope and Lmage-Pro Plus 6.0 are listed in Table II. It is noted that these primary I-phases exhibit an obvious characteristic of 5-fold symmetry in the samples, as showed in Fig. 2(d).

The compositions of I-phases in the $Mg_{57}Zn_{37}Y_6$ alloy solidified at various wheel speeds are determined by the EDS in SEM. The composition of the primary I-phase for all the investigated samples is in the range of $Mg_{28\text{-}34}Zn_{57\text{-}62}Y_{9\text{-}10}$ (at.%), which is very close to the composition ($Mg_{30}Zn_{60}Y_{10}$) reported by Luo et al.[3] According to the XRD pattern, SEM and EDS analyses, the petal-like phases could be preliminarily identified

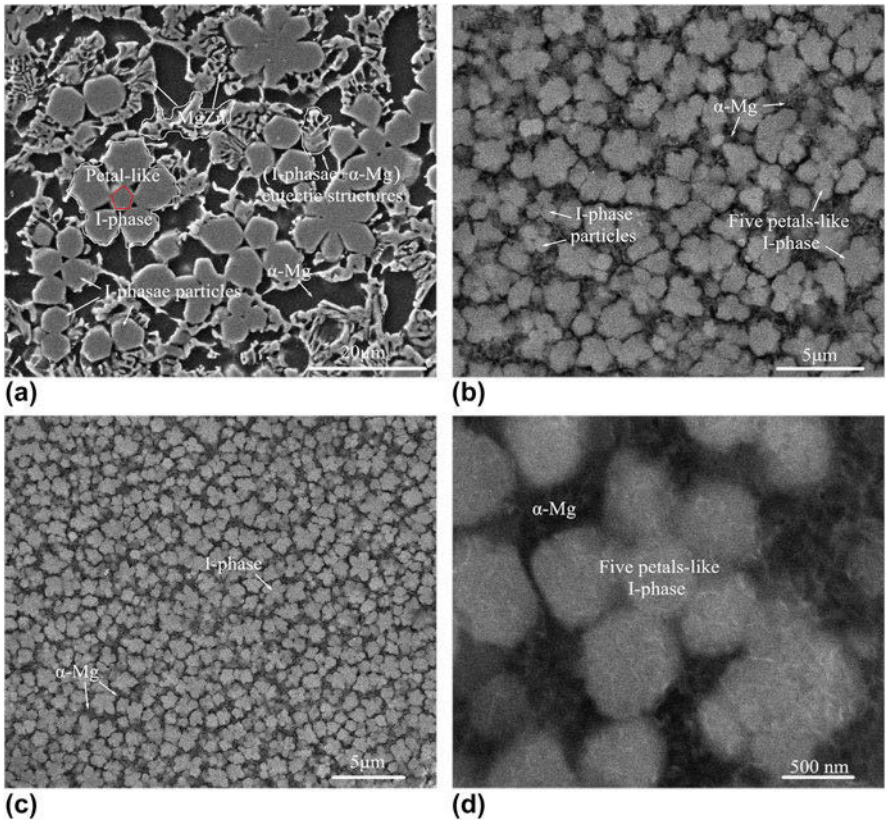

FIG. 2. Typical SEM images of the $Mg_{57}Zn_{37}Y_6$ alloy solidified at different wheel speeds. Overall morphology SEM image of conventionally-cast alloy (a) and 400 r/min (b); low (c) and high (d) magnification characteristic morphology of 800 r/min, respectively.

as icosahedral quasicrystals. TEM analysis is further used to accurately confirm the microstructures with a composition near to $Mg_{30}Zn_{60}Y_{10}$. The bright-field image and corresponding selected-area electron diffraction patterns of I-phases are shown in Fig. 3(a). The I-phase can be strongly identified according to the result of 5-fold axes in the composite selected-area electron diffraction patterns along the matrix hexagonal [111] axis. Figure 3(b) shows the EDS spectra from the points marked A and B in the bright-field image of Fig. 3(a). The I-phase is identified in the region A, where the composition is analyzed to be $Mg_{31.2}Zn_{59.6}Y_{9.2}$ (at.%). Position B is detected to be the matrix.

C. The effect of cooling rates on phase transition process of rapidly solidified $Mg_{57}Zn_{37}Y_6$ ribbons

The solidification path could be reconstructed from the DSC curve. Figure 4(a)–4(c) shows the DSC curves of the $Mg_{57}Zn_{37}Y_6$ alloys solidified at different cooling rates. As can be seen, DSC curve of conventionally-cast alloy demonstrates three obvious endothermic peaks, but only two endothermic peaks in the DSC curves of rapidly solidified $Mg_{57}Zn_{37}Y_6$ ribbons. The onset temperatures of the same endothermic peaks for three alloys decrease dramatically under a higher cooling rate. In addition, I-phase in Mg–Zn–Y alloy is generally supported to be formed by a peritectic reaction[25] (L + (Zn, Mg)$_5$Y → I-phase[26] or L + W-phase → I-phase[27]). However, although the cooling rates of the samples are different, the microstructures and corresponding DSC curves reveal that the primary I-phases of the $Mg_{57}Zn_{37}Y_6$ alloys solidified at different cooling rates can precipitate directly from the melt.

TABLE II. Average volume fraction and the grain size of I-phases of rapidly solidified $Mg_{57}Zn_{37}Y_6$ alloys at different wheel speeds.

Sample	Wheel speeds (r/min)	Volume fraction (%)	Grain size (μm)
As-cast alloy	0	29	17.0
Specimen 1	400	41	2.2
Specimen 2	800	53	1.3

In Fig. 4(a), three endothermic peaks occur at about 624, 473, and 335 °C, respectively during the heating process. According to the DSC curve, α-Mg precipitates from undercooled liquid firstly (about 624 °C). Then I-phase precipitates at around 473 °C directly from the melt. It can be seen from the DSC curves that the decomposition of icosahedral quasicrystals is a sluggish process. During the nucleation and growth of I-phase, the Y element plays a significant role. Previous investigations have shown that the pentagonal core forms from the melt as the icosahedral quasicrystal morphology in the region with Y concentration.[28] Subsequently, the Mg element is squeezed out to the edge of I-phase, and most Y element diffuses to supply the growth of I-phase. Practically, solute partitioning takes place at the solid/liquid interface attributing to the different diffusion of atoms and the atoms are most closely packed along the 5-fold axes, followed by 2-fold axes, as shown in Fig. 5.[29] Due to the fact that the 5-fold and 2-fold axes are the preferred growth orientations of the I-phase, the icosahedral quasicrystal should grow in its best preferred growth orientation along each 5-fold symmetry axis. Similar results were reported about decagonal quasicrystal phase in the $Al_{72}Ni_{12}Co_{16}$ alloy.[30] Each branch grows at a fastest rate along one 5-fold axis, which develops into a petal-like morphology eventually.

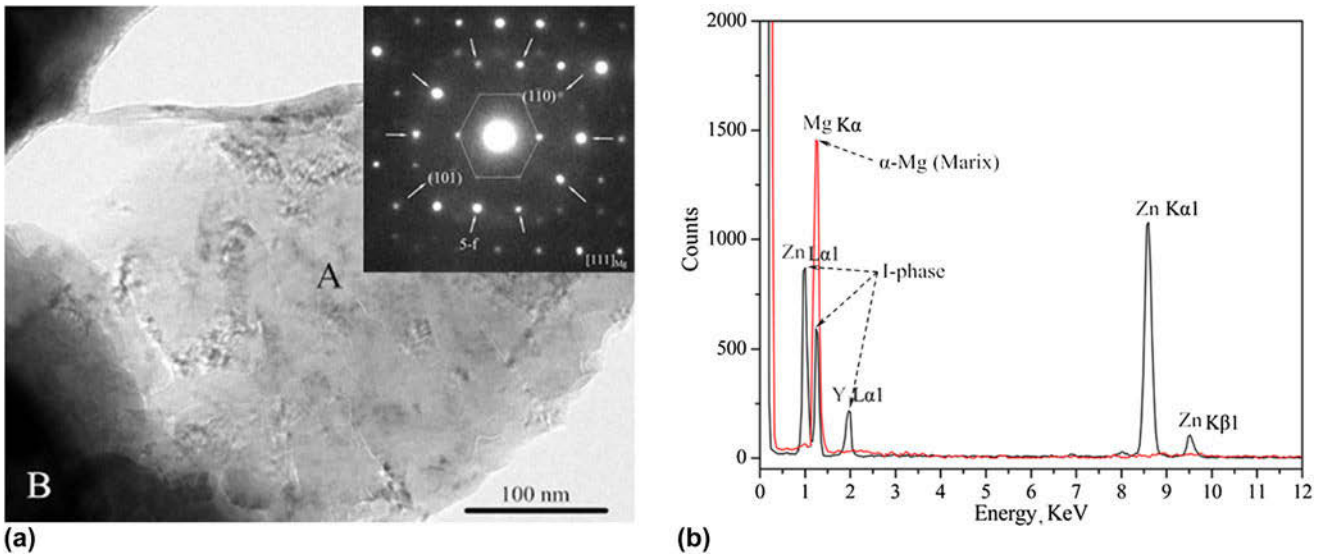

FIG. 3. (a) A bright-field TEM micrograph of I-phase and a composite selected area electron diffraction patterns along the matrix hexagonal [111] zone axis (marked with a hexagon), 5-fold axes marked by arrows, (b) EDS in TEM.

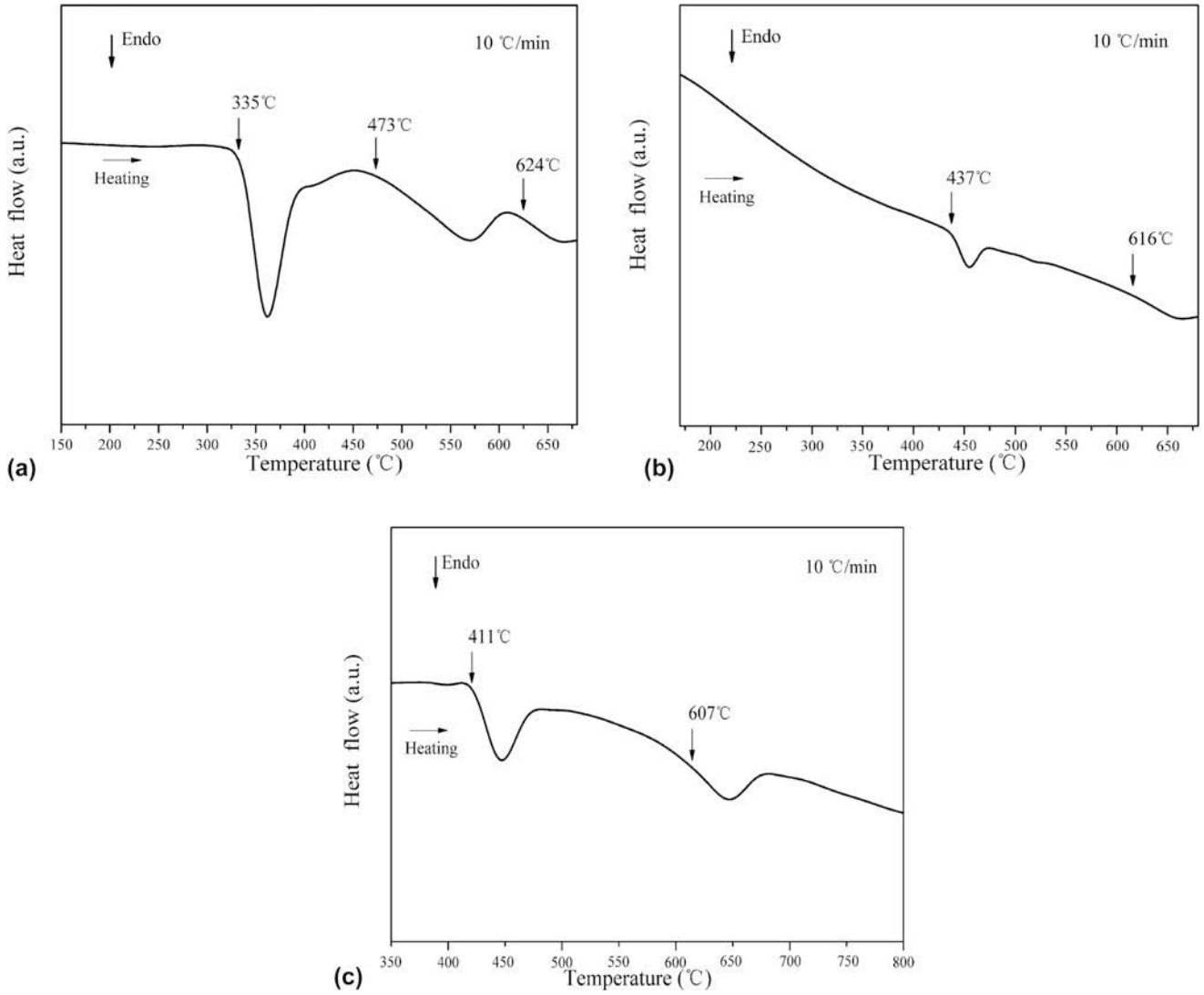

FIG. 4. DSC curves of the $Mg_{57}Zn_{37}Y_6$ alloy solidified at different wheel speeds: (a) conventionally-cast alloy, (b) 400 r/min, and (c) 800 r/min. For each curve, the corresponding phase transition temperatures are defined by arrows as the onset temperatures of the endothermic peaks, respectively.

In the case of Y element-free, low-temperature phase (MgZn) last solidifies from the remaining liquid at around 335 °C.

The MgZn phases are absent from the DSC curve of rapidly solidified $Mg_{57}Zn_{37}Y_6$ at wheel speeds both of 400 and 800 r/min, due to the fact that MgZn phases are low-temperature phases. It is commonly believed that the low-temperature phases of alloys are inhibited to nucleate in the stage of rapid solidification. Actually, the higher cooling rate allows a larger solid solubility of Zn in Mg,[16] which inhibits the formation MgZn phase during rapid solidification. Furthermore, the higher cooling rate leads to a large degree of supercooling, and further results in the phase transition temperature defined by arrows as the onset temperatures of the endothermic peaks, respectively, decreasing dramatically, as shown in Figs. 4(a)–4(c). The melting temperature directly drops down to icosahedral quasicrystal nucleation before primary nucleation of the crystal phase, achieving the thermodynamic conditions of quasicrystal nucleation.

In addition, recent studies have confirmed that the Icosahedral short-range order (ISRO) can contribute to forming quasicrystal phases.[31–34] When the liquid temperature is below a critical temperature (T_c), there are solid-like clusters or short-range orders existed in melt.[35] Icosahedral quasicrystals in Mg–Zn–RE are recognized as Tsai class consisting of four consecutive atomic shells, the third layer of which is icosahedron composed of 12 Y atoms, and the melting of quasicrystals is accompanied with formation of atomic clusters on the surface.[28,36] It is postulated that the short-range atomic clusters can evolve into ISROs with

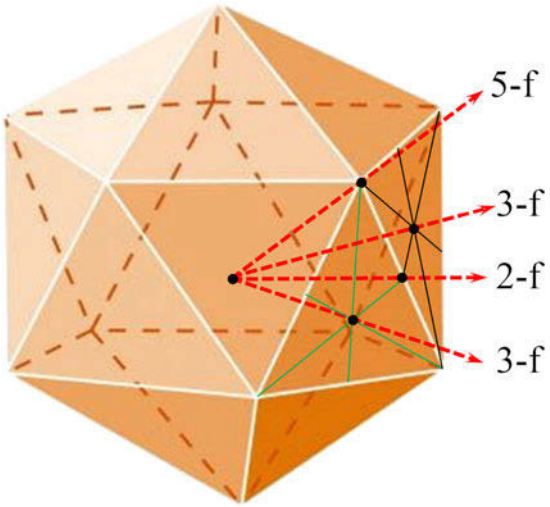

FIG. 5. An icosahedron model, 5-fold axes along the vertices; 3-fold axes perpendicular to equilateral triangle-shaped faces; 2-fold axes perpendicular to the edges.

the action of the Y element. Practically, ISRO exists widely in melts and can reunite large ISROs with the melt temperature decreasing. Hence, large region with ISROs will form in the initial stage of melting. The initial ISROs evolve into solid icosahedral clusters, which can be regarded as the start of the nucleation process of the I-phase. In addition, much larger size of icosahedral clusters or icosahedral local orderings for nucleation of I-phase is essential. So they connect along 5-fold directions followed by growth, which are the most stable coordination manner demonstrated by Egami.[37]

With the increasing cooling rate, the ISROs are more easily arrested, which causes the higher survival probability of icosahedral clusters during the rapid quenching than the as-cast one. The higher cooling rate can contribute to a large degree of supercooling, and result in a large number of ISROs, which are conducive to precipitate directly from the melt for icosahedral quasicrystals. However, the detailed coordination models among the icosahedral clusters in the melt and their heredities from liquid to solid require a further investigation.

Furthermore, much more I-phases with a smaller size indicate that large numbers of nucleation embryos are promoted by a large degree of supercooling. Meanwhile, there is no enough time for the atomic diffusion and solute reallocation. The solute partitioning and local overheating therefore cannot occur, which makes the microstructure more homogeneous that is consistent with the result shown in Fig. 2.

IV. CONCLUSIONS

The effect of cooling rates on solidification and microstructure of rapidly solidified $Mg_{57}Zn_{37}Y_6$ (at.%) quasicrystal alloy was studied. It is found that:

(1) With the increasing cooling rate, the thickness of the ribbon decreases greatly. The decrease in the thickness of the ribbon can be attributed to the more rapid movement of the liquid.

(2) Rapid solidification changes the phase constitution of $Mg_{57}Zn_{37}Y_6$ alloy. α-Mg, MgZn, and icosahedral phase coexist in the as-cast Mg–Zn–Y alloy, but MgZn phase is absent from rapidly solidified alloy. The microstructure is refined and uniform under a higher cooling rate, and the higher the cooling rate, the more the amount of I-phase is retained.

(3) Icosahedral quasicrystals are successfully prepared under different cooling rates. It is revealed that the I-phase can precipitate directly from the melt during the solidification process. A higher cooling rate leads to a large degree of supercooling, and further results in the decreased phase transition temperature.

ACKNOWLEDGMENTS

The financial support for this work is provided by the National Natural Science Foundation of China (No. 51571102) and the Special Joint Funds of Natural Science Foundation of Shandong Province, China (ZR2013EML004).

REFERENCES

1. K. Hono, C.L. Mendis, T.T. Sasaki, and K. Oh-ishi: Towards the development of heat-treatable high-strength wrought Mg alloys. *Scr. Mater.* **63**, 710 (2010).
2. D. Shechtman, I. Blech, D. Gratias, and J.W. Cahn: Metallic phase with long-range orientational order and no translational symmetry. *Phys. Rev. Lett.* **53**, 1951 (1984).
3. Z.P. Luo, S.Q. Zhang, Y.L. Tang, and D.S. Zhao: Quasicrystals in as-cast Mg–Zn–RE alloys. *Scr. Metall. Mater.* **28**, 1513 (1993).
4. A.P. Tsai, A. Niikura, A. Inoue, and T. Masumoto: Stoichiometric icosahedral phase in the Zn–Mg–Y system. *J. Mater. Res.* **12**, 1468 (1997).
5. M. Wollgarten, M. Beyss, and K. Urban: Direct evidence for plastic deformation of quasicrystals by means of a dislocation mechanism. *Phys. Rev. Lett.* **71**, 549 (1993).
6. S. Takeuchi, H. Iwanaga, and T. Shibuya: Hardness of quasicrystals. *Jpn. J. Appl. Phys.* **30**, 561 (1991).
7. J.M. Dubois, S.S. Kang, and J. von Stebut: Quasicrystalline low-friction coatings. *J. Mater. Sci. Lett.* **10**, 537 (1991).
8. T. Yoshida, K. Itoh, R. Tamura, and S. Takeuchi: Plastic deformation and hardness in Mg-Zn-(Y, Ho) icosahedral quasicrystals. *Mater. Sci. Eng., A* **786**, 294 (2000).
9. W. Yang, F. Liu, H.F. Wang, B.P. Lu, and G.C. Yang: Non-equilibrium transformation kinetics and primary grain size distribution in the rapid solidification of Fe–B hypereutectic alloy. *J. Alloys Compd.* **509**(6), 2903 (2011).
10. E.J. Lavernia and T.S. Srivatsan: The rapid solidification processing of materials: Science, principles, technology, advances, and applications. *J. Mater. Sci.* **45**(2), 287 (2010).
11. M. Gogebakan, O. Uzun, T. Karaaslan, and M. Keskin: Rapidly solidified Al-6.5 wt.% Ni alloy. *J. Mater. Process. Technol.* **142**(1), 87 (2003).

12. X.F. Guo and D. Shechtman: Extruded high-strength solid materials based on magnesium with zinc, yttrium, and cerium additives. *Glass Phys. Chem.* **31**(1), 44 (2005).
13. S.W. Lee, H.Y. Wang, Y.L. Chen, J.W. Yeh, and C.F. Yang: An Mg–Al–Zn alloy with very high specific strength and superior high-strain-rate superplasticity processed by reciprocating extrusion. *Adv. Eng. Mater.* **6**(12), 948 (2004).
14. D.Q. Wan, G.C. Yang, L. Lin, and Z.G. Feng: Equilibrium and non-equilibrium microstructures of Mg–Zn–Y quasicrystal alloy. *Mater. Lett.* **62**, 1711 (2008).
15. S. Yi, E.S. Park, J.B. Ok, W.T. Kim, and D.H. Kim: (Icosahedral phase + α-Mg) two phase microstructures in the Mg–Zn–Y ternary system. *Mater. Sci. Eng., A* **300**, 312 (2001).
16. Z.M. Zhang, C.J. Xu, and X.F. Guo: Microstructure of Mg-6.4Zn-1.1Y alloy fabrication by rapid solidification and reciprocating extrusion. *Acta Metall. Sin. (Engl. Lett.)* **21**, 30 (2008).
17. Z.G. Liu, L.H. Chai, and Y.Y. Chen: Effect of cooling rate and Y element on the microstructure of rapidly solidified TiAl alloys. *J. Alloys Compd.* **504**, 491 (2010).
18. J.W. Geng, X.Y. Teng, G.R. Zhou, and Z.W. Zhao: Solidification and microstructure of as-cast $Mg_{65}Zn_{32}Y_3$ quasicrystal alloy. *Phys. B* **420**, 64 (2013).
19. C.R. Li, N.P. Lu, Q. Xu, J. Mei, W.J. Dong, J.L. Fu, and Z.X. Cao: Decahedral and icosahedral twin crystals of silver: Formation and morphology evolution. *J. Cryst. Growth* **319**, 88 (2011).
20. M.A. Taha: Geometry of melt-spun ribbons. *Mater. Sci. Eng., A* **134**, 1162 (1991).
21. B. Cantor, W.T. Kim, B.P. Bewlay, and A.G. Gillen: Microstructure-cooling rate correlations in melt-spun alloys. *J. Mater. Sci.* **26**(5), 1266 (1991).
22. A.G. Gillen and B. Cantor: Photocalorimetric cooling rate measurements on a Ni-5wt.% Al alloy rapidly solidified by melt spinning. *Acta Metall.* **33**(10), 1813 (1985).
23. G. Liu, Z.Z. Zhang, Q. Chen, H. Zhang, C.H. Yin, and S.M. Zhang: Microstructures and properties of rapidly solidified Mg–Zn–Y–Zr alloy ribbons. *Mater. Eng.* **9**, 38 (2009). [In Chinese].
24. J.W. Geng, X.Y. Teng, G.R. Zhou, D.G. Zhao, and J.F. Leng: Growth mechanism of an icosahedral quasicrystal and solute partitioning in a Mg-rich Mg–Zn–Y alloy. *J. Mater. Res.* **29**, 942 (2014).
25. F. Shi, X.F. Guo, and Z.M. Zhang: Study on the quasicrytal phase in $Mg_{74}Zn_{25}Y_1$ alloy. *Chin. J. Mech. Eng.* **39**(8), 138 (2003).
26. M.R. Li and K.H. Kuo: Intermetallic phases and phase reactions in Zn–Mg (<40 at.%)-Y (<20 at.%) region. *J. Alloys Compd.* **432**, 81 (2007).
27. J.B. Ok, I.J. Kim, S. Yi, T.W. Kim, and D.H. Kim: Solidification microstructure of as-cast Mg–Zn–Y alloys. *Philos. Mag. A* **83**, 2359 (2003).
28. S. Ranganathan and A. Inoue: An application of Pettifor structure maps for the identification of pseudo-binary quasicrystalline intermetallics. *Acta Mater.* **54**, 3647 (2006).
29. K. Chattopadhyay, N. Ravishankar, and R. Goswami: Shapes of quasicrystals. *Prog. Cryst. Growth Charact. Mater.* **34**, 237 (1997).
30. Y.C. Liu, G.C. Yang, Y.H. Zhou, T. Wang, D.S. Xu, and Q.Y. Xu: Growth mode of decagonal quasicrystal phase in laser resolidified $Al_{72}Ni_{12}Co_{16}$ alloy. *J. Cryst. Growth* **207**, 292 (1999).
31. H. Klein, M. Audier, V. Simonet, F. Hippert, and R. Bellissent: Icosahedral order in a liquid metallic alloy: Molten AlPdMn quasicrystal. *Phys. B* **964**, 241 (1998).
32. D. Holland-Moritz, J. Schroers, D.M. Herlach, B. Grushko, and K. Urban: Undercooling and solidification behaviour of melts of the quasicrystal-forming alloys Al–Cu–Fe and Al–Cu–Co. *Acta Mater.* **46**(5), 1601 (1998).
33. O.S. Roik, S.M. Galushko, O.V. Samsonnikov, V.P. Kazimirov, and V.E. Sokolskii: Structure of liquid Al–Cu–Co alloys near the quasicrystal-forming range. *J. Non-Cryst. Solids* **357**, 1147 (2011).
34. J.W. Geng, X.Y. Teng, G.R. Zhou, and D.G. Zhao: Temperature dependence of the electrical resistivity of Mg–Zn–Y quasicrystal alloy. *Mater. Lett.* **132**, 334 (2014).
35. S.L. Ye, X.Y. Li, X.F. Bian, W.M. Wang, and L.J. Yin: Remelting treatment and heredity phenomenon in the formation of $Fe_{78}Si_9B_{13}$ amorphous alloy. *J. Alloys Compd.* **562**, 143 (2013).
36. V.E. Dmitrienko, S.B. Astaf'ev, and M. Kléman: Growth, melting, and clustering of icosahedral quasicrystals: Monte Carlo simulations. *Mater. Sci. Eng., A* **294–296**, 413 (2000).
37. T. Egami: Icosahedral order in liquids. *J. Non-Cryst. Solids* **353**, 3666 (2007).